PACS 73.40.Ns, 73.40.Cg, 85.40.-e

On a feature of temperature dependence of contact resistivity for ohmic contacts to *n*-Si with an n^+-*n* doping step

A.V. Sachenko[1], A.E. Belyaev[1], N.S. Boltovets[2], A.O. Vinogradov[1], V.A. Pilipenko[3], T.V. Petlitskaya[3], V.M. Anischik[4], R.V. Konakova[1], T.V. Korostinskaya[2], V.P. Kostylyov[1], Ya.Ya. Kudryk[1], V.G. Lyapin[1], P.N. Romanets[1], V.N. Sheremet[1]
[1]V. Lashkaryov Institute of Semiconductor Physics, NAS of Ukraine, 03028 Kyiv, Ukraine
Phone: 38(044) 525-61-82; Fax: 38(044) 525-83-42; e-mail: konakova@isp.kiev.ua
[2]State Enterprise Research Institute "Orion", 03057 Kyiv, Ukraine
[3]State Centre "Belmicroanaliz", subsidiary of R&D Centre "Belmicrosystems"
Open Joint Stock Company "Integral", 220108 Minsk, Belarus
[4]Belarusian State University, 220030 Minsk, Belarus

Abstract. We present both theoretical and experimental temperature dependences of contact resistivity $\rho_c(T)$ for ohmic contacts to the silicon n^+-*n*-structures whose n^+-layer was formed using phosphorus diffusion or ion implantation. The $\rho_c(T)$ dependence was measured in the 125–375 K temperature range with the transmission line method, with allowance made for conduction in both the n^+-layer and n^+-*n* doping step.

Keywords: ohmic contact, metallization, doping step.

Manuscript received 24.10.13; revised version received 11.12.13; accepted for publication 20.03.14; published online 31.03.14.

1. Introduction

At present there exists a fixed notion of the mechanisms of current flow in ohmic metal-semiconductor contacts as well as the processes of minimization of contact resistivity and their contribution to the parameters of semiconductor devices and integrated circuits [1]. This notion asserts that contact resistivity ρ_c should be minimal and demonstrate thermal and electrical stability, and $I - V$ curves of ohmic contacts must be linear and symmetric. As a rule, ρ_c of such contacts is described within either field emission (ρ_c does not depend on temperature) or thermofield emission (ρ_c decreases with temperature).

However, recent investigations [2-9] showed that in some cases ρ_c does not demonstrate the above behavior. To illustrate, for ohmic contacts to wide-gap semiconductors with high dislocation density it was shown in [2-4, 8, 9] that ρ_c increases with temperature. Such growing dependences $\rho_c(T)$ were obtained in [5-7] for ohmic contacts to lapped as well as polished *n*-Si, at presence of high density of structural defects in the Si near-contact region. In that case, calculation of the number of defects from etching pits made for lapped silicon gave ~10^7 cm^{-2}. According to the model proposed in [7, 8], this value turned out sufficient for description of growing dependence $\rho_c(T)$.

Along with the above-mentioned, some other conditions of ohmic contact formation may lead to ρ_c growth with temperature. For instance, use (as an ohmic contact) of an isotype n^+-*n* junction (n^+-*n* doping step) or p^+-*p* junction – analog of metal-semiconductor contact in which degenerate n^+-semiconductor (or p^+-semiconductor) acts as a metal. In this case, we deal practically with a Schottky diode without a potential barrier [10]. In what follows, we consider a model of such ohmic contact and its experimental testing.

© 2014, V. Lashkaryov Institute of Semiconductor Physics, National Academy of Sciences of Ukraine

2. Model of ohmic contact with a doping step

Let us consider a model of ohmic contact with an n^+-n doping step in the near-contact region, with electrons in the heavily doped n^+-layer being degenerate. This situation is realized in manufacturing technology for silicon devices, in particular, IMPATT diodes. In that case, the thickness W_{n^+} of the heavily doped region with electron concentration n_1^+ exceeds the Schottky layer thickness W_{Sh}, and the doping level is over the effective density of states N_c in the conduction band. Just this situation means that electrons in the heavily doped region are degenerate.

In this work, we made an analytical calculation of the $\rho_c(T)$ curve for Si-based ohmic contacts with an n^+-n doping step in the limiting case when the contact band diagram is of the form shown in Fig. 1. One can see that the thickness W_{n^+} of the heavily doped region with electron concentration n_1^+ exceeds the Schottky layer thickness W_{Sh} ($W_{n^+} > W_{\text{Sh}}$), and the doping level exceeds the effective electron density of states in the conduction band N_c ($n_1^+ > N_c$). This means that electrons in the heavily doped region are degenerate.

Figs 2a and 2b present band diagrams for contacts to Si with a doping step, at two values of heavily doped layer thickness W_{n^+}: 5 and 10 nm. In our calculations, we used the following values: $n_2 = 10^{16}\,\text{cm}^{-3}$, $n_1^+ =$ $2\cdot10^{18}$, $5\cdot10^{18}$, 10^{19}, $2\cdot10^{19}$ and $5\cdot10^{19}\,\text{cm}^{-3}$. To obtain the band diagrams, we solved the Poisson equations for the heavily doped and lightly doped regions (both with allowance made for electron degeneracy) of the form

$$\frac{d^2\varphi}{dx^2} = \frac{1}{\varepsilon_0\varepsilon_s}\rho(x), \tag{1}$$

where

$$\rho(x) = q\left[\frac{8\pi\left(m_p T\right)^{3/2}}{\left(2\pi\hbar\right)^3}\int_0^\infty dz \frac{z^{1/2}}{\exp\left(z - \frac{E_F - q\varphi}{kT}\right)+1} - \frac{n_1{}^+\theta\left(W_{n^+} - x\right) + n_2\theta\left(x - W_{n^+}\right)}{\exp\left(\frac{E_a + E_F - q\varphi}{kT}\right)}\right]. \tag{2}$$

Here E_F is the Fermi energy, $E_a \approx 0.005$ eV, q – elementary charge.

The barrier height at the contact (or, more exactly, the diffusion potential φ_c) was preset as 0.4 V. The electrostatic potential was considered to vanish as $x\to\infty$. The solutions of the Poisson equation in the heavily and lightly doped regions were matched at the boundary $x = W_{n^+}$, that is to say, the values of potentials, as well as their derivatives (i.e., the electric field strengths), were matched, respectively.

Naturally all the n_1^+ values taken for calculation obeyed the inequality $n_1^+ > N_c$. However, since the Schottky layer thicknesses in the heavily doped region met the condition $W_{n^+} < W_{\text{Sh}}$ at all doping levels, there

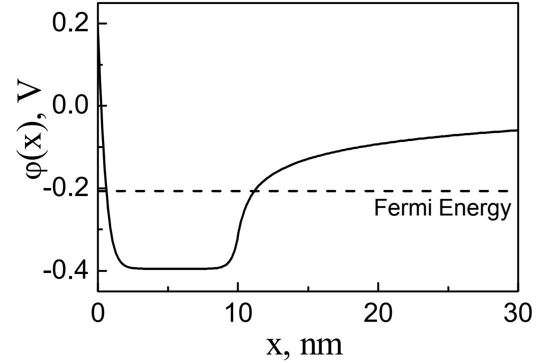

Fig. 1. Band diagram of ohmic contact with an n^+-n doping step; $n^+\sim 5\cdot10^{20}$ cm^{-3}; $n \sim 10^{16}$ cm^{-3}; $W_{n+}\sim 0.01$ µm.

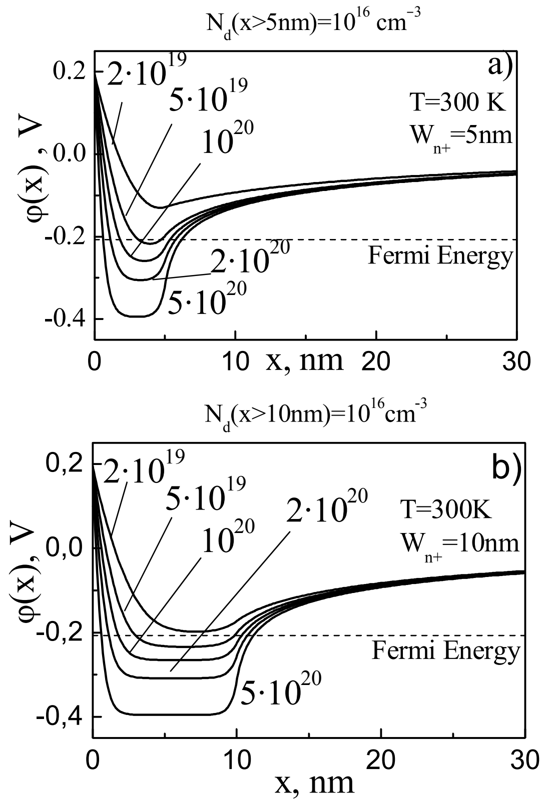

Fig. 2. Band diagrams of contacts with a doping step for Si at two thickness values of heavily doped layer W_{n+}: 5 nm (*a*) and 10 nm (*b*); n^+: $5\cdot10^{19}$, 10^{20}, $2\cdot10^{20}$ and $5\cdot10^{20}$ cm^{-3} at $n_2 = 10^{16}$ cm^{-3}.

© 2014, V. Lashkaryov Institute of Semiconductor Physics, National Academy of Sciences of Ukraine

was no portion of $\varphi(x)$ independent from the coordinate x shown in Fig. 1.

One should note that, depending on the behavior of potential $\varphi(x)$ in the near-contact region, the contact will be either rectifying (in the case of monotonic dependence of $\varphi(x)$ on coordinate x) or ohmic (in the case of a strongly pronounced non-monotony of $\varphi(x)$). In the latter case, the contact resistivity may be presented as a sum of two terms (corresponding to series resistances):

$$\rho_c = \rho_{c1} + \rho_{c2}\,. \quad (3)$$

Here, ρ_{c1} is the contact resistivity related to thermofield passage of electrons through the barrier at the interface between a heavily doped semiconductor and metal, and

$$\rho_{c2} = \frac{k N_c}{q A^* T n_2}\left(1 + \frac{L_D A^* T}{k \mu_n N_c}\right) \quad (4)$$

is the effective contact resistance of the lightly doped region in the limiting case of contact energy band being of the form shown in Fig. 1. Here k is the Boltzmann constant, A^* – effective Richardson constant, μ_n – electron mobility in the lightly doped region, $L_D = (\varepsilon_0 \varepsilon_s kT / 2q^2 n_2)^{0.5}$ – Debye shielding length for the lightly doped region. It should be noted that Eq. (4) was obtained with allowance made for the results of [10] and [11]: it takes into account both the diffusion and emission terms in the current flowing through the lightly doped region.

Thus, if the inequality $\rho_{c2} > \rho_{c1}$ holds, then contact is purely ohmic. In that case, band bending in the lightly doped region is accumulation rather than depletion, so the total voltage applied to the contact is dropped across the neutral bulk, thus ensuring contact ohmicity. The electron mobility μ_n in the region of light doping was calculated with allowance made for electron scattering by charged impurities as well as by intervalley and acoustic phonons [12]. It was assumed that dislocation density in the lightly doped region is sufficiently low and does not affect electron mobility. The expressions for μ_n calculation are given in [8].

Now let us dwell on an analysis of temperature dependence of contact resistivity ρ_{c2}. If the role of diffusion current is insignificant (that is to say, the inequality $((L_D A^* T) / (k\,\mu_n N_c)) < 1$ holds), then one obtains with allowance made for $N_c(T) = N_{c0}(T/300\text{ K})^{3/2}$ that $\rho_{c2} \sim \sqrt{T}$, i.e., the contact resistivity grows with temperature as $\sqrt{T}$. It was shown in [10] that the above inequality is valid at doping levels $n_2 >> 10^{15}$ cm^{-3}. At lower and intermediate doping levels, $((L_D A^* T) / (k\,\mu_n N_c)) \geq 1$, and (as analysis shows) the degree of ρ_{c2} growth with temperature increases as compared with the law $\sqrt{T}$.

Fig. 3 presents the theoretical $\rho_{c2}(T)$ curves built using Eq. (4) as well as low-temperature freeze-out of electrons. The doping level serves as parameter of curves. At temperatures over 125 K, all curves grow with temperature (see curves *1-3*). For the curve *1* (that corresponds to the lowest doping level of $10^{14}\,\text{cm}^{-3}$), the exponent of the power dependence $\rho_{c2}(T)$ at room and elevated temperatures is maximal (equal to 2). As the doping level increases, that exponent goes down: it equals 1.1 at $n_2 = 10^{15}\,\text{cm}^{-3}$ and 0.8 at $n_2 = 10^{16}\,\text{cm}^{-3}$.

It should be noted that the above current mechanism (as well as that related to current flow through the metal shunts associated with dislocations – see [7, 8]) ensures purely ohmic contact behavior. At the same time, the standard mechanism that describes slightly non-ohmic contact with low barrier height (about kT/q), as well as the thermofield mechanism of current flow, result in ohmic contact behavior only in the case that $R_c > R_b$ (here R_c is the contact resistance, and R_b is the bulk resistance). Let us assume that the thermofield current component is predominant over wide ranges of doping levels and temperatures. Then, it is possible to use the following equation for determination of $I-V$ curve for a contact of unit area:

$$J(V) = J_{sT}\left[\exp\left(\frac{q(V - JR_b)}{E_0}\right) - 1\right], \quad (5)$$

where

$$J_{sT} = \frac{E_0}{q} R_{tp}^{-1}\,;\; E_0 = E_{00}\,\text{cth}(E_{00}/kT)\,;$$

$$E_{00} = \hbar / 2(\varepsilon_0 \varepsilon_s m_t / n)^{1/2}\,. \quad (6)$$

Here, $R_{tp} = \rho_{tp} / S$ (where ρ_{tp} is contact resistivity at realization of thermofield mechanism of current flow through the contact), S is the contact area.

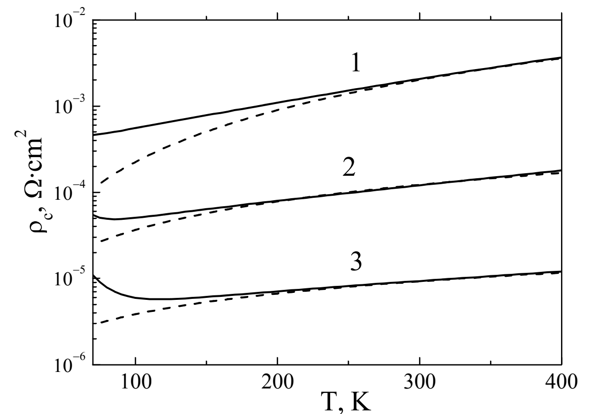

Fig. 3. Theoretical $\rho_{c2}(T)$ curves built using Eq. (4) (full curves) and with allowance made for low-temperature freeze-out of electrons (dashed curves; n_2, cm^{-3}: *1* – 10^{14}; *2* – 10^{15}; *3* – 10^{16}).

© 2014, V. Lashkaryov Institute of Semiconductor Physics, National Academy of Sciences of Ukraine

By presenting the I–V curve as

$$J(V) = \frac{V}{R_b} - \frac{E_0}{qR_b} \ln\left(1 + \frac{J}{J_{sT}}\right), \quad (7)$$

it is easy to make certain that the second term on the right of Eq. (7) may be neglected as compared to the first one if $R_{tp} << R_b$. To this end, as it follows from Eq. (7), the inequality $J << J_{sT}$ has to hold. Then, using the expression for J_{sT} from Eq. (6), we obtain

$$J(V) = \frac{V}{R_b} - J(V)\frac{R_{tp}}{R_b}. \quad (8)$$

One can see from this that condition for contact ohmicity is $R_{tp} << R_b$.

3. Details of experiment

We studied two types of specimens, with an n^+-n doping step formed either by phosphorus diffusion or ion implantation, at identical n-Si(111) wafers. The latter were cut out of the same ingot made by the Czochralski method. Their thickness and resistivity were ~420 µm and ~4.6 Ω·cm, respectively. The wafers were subjected to chemo-dynamical polishing and surfaced according to the requirements of the 14th class.

Phosphorus diffusion from vapor phase was made at T = 900 °C for 6 min. The depth of occurrence of the n^+-layer was ~0.065 µm; the donor concentration in the n^+-layer was $\sim 10^{20}\,\text{cm}^{-3}$. Phosphorus ion implantation was made using a setup “Vesuvius–5”. The ion energy was ~60 keV; the dose was 10^3 µC/cm^2. Thermal annealing after ion implantation was made using a setup “SDOM 3–100” in oxygen atmosphere at T = 850 °C for 30 min. The depth of occurrence of the n^+-layer was ~0.06 µm. The surface concentration of the dopant was $\sim 10^{15}\,\text{cm}^{-2}$.

To measure $\rho_c(T)$ over the 125–375 K temperature range, we made test structures with specimens of both types. The configuration of test structures corresponded to ρ_c measurement with the transmission line method (TLM) [13] that was used by us earlier in [5-8]. It enabled us to test ρ_c with allowance for either conduction in the n^+-layer only (planar configuration of TLM structure) or through the n^+-n doping step (vertical configuration of TLM structure). In the latter case, vertical TLM structure was made by n^+-layer etching-off in gaps between the test pads to a depth of ~0.5 µm and 1 µm, respectively, i.e., much over the thickness of n^+-layer.

Contact metallization Au(150 nm)–Ti(60 nm)–Pd(20 nm)–n^+-n was made using layer-by-layer vacuum sputtering of metals onto the Si substrate (heated to 350 °C) with an n^+-n doping step, in a single technological cycle, in an oilless vacuum (residual pressure of $\sim 5 \cdot 10^{-4}\,\text{Pa}$). The opposite wafer side was metallized in much the same way.

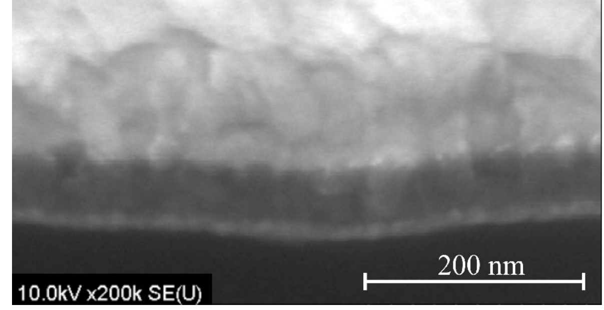

Fig. 4. SEM microphotograph of the cleavage of Au–Ti–Pd–n^+-n-Si contact structure for an n^+-n doping step made using phosphorus diffusion.

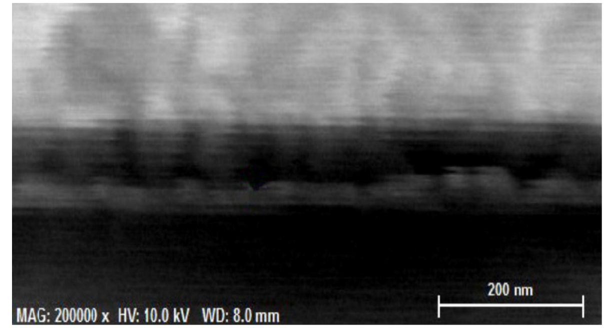

Fig. 5. Same as in Fig. 4 but for an n^+-n doping step made using phosphorus ion implantation.

For contact structures of both configurations, the cleavage surface was studied using a high resolution scanning electron microscope (SEM) S–4800 (Hitachi, Japan).

The SEM photographs of cleavages for Au–Ti–Pd–n^+-n-Si structures with an n^+-layer prepared using phosphorus diffusion and ion implantation are shown in Figs 4 and 5, respectively. In both photographs, one can see n^+-n doping steps with practically close n^+-layer thicknesses.

4. Experimental results: Comparison with the model

Shown in Fig. 6 are the dependences $\rho_c(T)$ measured over the 125–375 K temperature range for specimens of two types: 1) with an n^+-n doping step obtained using phosphorus ion implantation into a silicon wafer (ρ ~4.6 Ω·cm) and 2) with an n^+-n doping step obtained using phosphorus diffusion into the same Si wafer. The dependences $\rho_c(T)$ presented in Fig. 6 were measured in two ways: 1) at lateral current flow in the n^+-layer and 2) at vertical current flow through the n^+-n doping step.

© 2014, V. Lashkaryov Institute of Semiconductor Physics, National Academy of Sciences of Ukraine

One can see from Fig. 6 (curves *1* and *1′*) that, at current flow in the n^+-layer (regardless of the way of its formation), the contact resistivity ρ_c grows with temperature but slightly (closely to dependence $\rho_c \sim T^{0.1}$ or $\rho_c \sim T^{0.2}$). The ρ_c value for the specimen with an ion-implanted n^+-layer is about 1/3 that for the specimen with n^+-layer obtained using phosphorus diffusion. This may be owing to the known advantages of the ion implantation method over the diffusion one [14].

The theoretical temperature dependence of contact resistivity is shown in Fig. 6 (curve 2), while the experimental $\rho_c(T)$ curve (obtained for diffusion-doped structure) is presented in Fig. 6 (curve 3); both curves are given for vertical geometry of TLM structure. One can see that there is no agreement between the above two curves. In our opinion, the reason for this is related to pronounced difference between the shunt and contact resistances. In our case, the shunt resistance value $R_{\rm Sh}$ exceeds that of contact resistance $R_c = \rho_c / S$ (where S is the contact area) by more than two orders of magnitude. So, the relative error in determination of contact resistance $\Delta\rho_c/\rho_c$ with the Cox and Strack method [15] is close to 100%. The results of calculation for vertical geometry of TLM structure show that, to decrease the ratio $R_{\rm Sh}/R_c$, one should use structures of smaller both diameter (~20 µm) and thickness (≤10 µm). This consideration will be taken into account later.

However, the principal result obtained in this work is that the $\rho_c(T)$ curves for vertical structures with a doping step are growing. This is related (as was showed above) to realization of accumulation band bending in a lightly doped region at the interface between the silicon bulk and doping step. This means that in this case we deal with purely ohmic contacts for which linear dependence between the flowing current and applied voltage is obeyed at any temperatures, whatever the interrelation between the bulk and contact resistances.

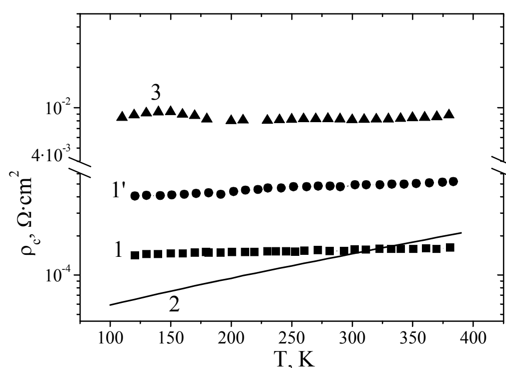

Fig. 6. Experimental temperature dependence of contact resistivity (planar geometry of TLM structure): 1 – ion implanted n^+-layer; 1′ – diffusion-doped n^+-layer; theoretical (2) and experimental (3) temperature dependences of contact resistivity at $n_2 = 8.5\times10^{14}$ cm^{-3} (vertical geometry of TLM structure).

5. Conclusions

Thus, it has been shown (both theoretically and experimentally) for ohmic contacts formed to an n^+-n doping step of silicon that, in the case of electron degeneracy in the n^+-layer and high-resistance n-Si bulk, contact resistivity ρ_c increases with temperature in the 125–375 K range. It is shown that the growing dependences $\rho_c(T)$ are related to the accumulation band bending in high-resistance n-Si, no matter what the way of formation (diffusion or ion implantation) of n^+-n doping step.

Acknowledgement

The work was supported by the Project №Ф54/209-2013 ДФФД–БРФФД–2013.

References

1. S.M. Sze, Kwok K. Ng, *Physics of Semiconductor Devices*. 3rd Ed. John Wiley and Sons, Inc., Hoboken, New Jersey, 2007.
2. T.V. Blank, Yu.A. Gol'dberg, Mechanisms of current flow in metal-semiconductor ohmic contacts // *Semiconductors*, **41**(11), p. 1263-1292 (2007).
3. Zhang Yue-Zong, Feng Shi-Wei, Guo Chun-Sheng, Zhang Guang-Chen, Zhuang Si-Xiang, Su Rong, Bai Yun-Xia, Lu Chang-Zhi, High-temperature characteristics of Ti/Al/Ni/Au ohmic contacts to *n*-GaN // *Chin. Phys. Lett.* **25**(11), p. 4083-4085 (2008).
4. T.V. Blank, Yu.A. Gol'dberg, A.E. Posse, Flow of the current along metallic shunts in ohmic contacts to wide-gap III–V semiconductors // *Semiconductors*, **43**(9), p. 1164-1169 (2009).
5. A.E. Belyaev, N.S. Boltovets, R.V. Konakova, Ya.Ya. Kudryk, A.V. Sachenko, V.N. Sheremet, Temperature dependence of contact resistance of Au–Ti–Pd_2Si–n^+-Si ohmic contacts // *Semiconductor Physics, Quantum Electronics and Optoelectronics*, **13**(4), p. 436-438 (2010).
6. A.E. Belyaev, N.S. Boltovets, R.V. Konakova, Ya.Ya. Kudryk, A.V. Sachenko, V.N. Sheremet, A.O. Vinogradov, Temperature dependence of contact resistance for Au–Ti–Pd_2Si–n^+-Si ohmic contacts subjected to microwave irradiation // *Semiconductors*, **46**(3), p. 330-333 (2012).
7. A.V. Sachenko, A.E. Belyaev, N.S. Boltovets, A.O. Vinogradov, V.P. Kladko, R.V. Konakova, Ya.Ya. Kudryk, A.V. Kuchuk, V.N. Sheremet, S.A. Vitusevich, Features of temperature dependence of contact resistivity in ohmic contact on lapped *n*-Si // *J. Appl. Phys.* **112**(6), 063703 (2012).
8. A.V. Sachenko, A.E. Belyaev, N.S. Boltovets, R.V. Konakova, Ya.Ya. Kudryk, S.V. Novitskii, V.N. Sheremet, J. Li, S.A. Vitusevich, Mechanism

© 2014, V. Lashkaryov Institute of Semiconductor Physics, National Academy of Sciences of Ukraine

of contact resistance formation in ohmic contacts with high dislocation density // *J. Appl. Phys*. **111**(8), 083701 (2012).

9. F. Iucolano, G. Greco, F. Roccaforte, Correlation between microstructure and temperature dependent electrical behavior of annealed Ti/Al/Ni/Au ohmic contacts to AlGaN/GaN heterostructures // *Appl. Phys. Lett*. **103**(20), 201604 (2013).
10. R.K. Kupka, W.A. Anderson, Minimal ohmic contact resistance limits to *n*-type semiconductors // *J. Appl. Phys*. **69**(6), p. 3623-3632 (1991).
11. G. Brezeanu, C. Cabuz, D. Dascalu, P.A. Dan, A computer method for the characterization of surface-layer ohmic contacts // *Solid-State Electron*. **30**(5), p. 527-532 (1987).
12. D.K. Ferry, First-order optical and intervalley scattering in semiconductors // *Phys. Rev. B*, **14**(4), p. 1605-1609 (1976).
13. D.K. Schroder, *Semiconductor Materials and Devices Characterization*. 3rd Ed., John Wiley and Sons, Inc., Hoboken, New Jersey, 2006.
14. *Ion Implantation and Beam Processing*, Eds. J.S. Williams, J.M. Poate. Academic Press, N.Y., 1984.
15. R.H. Cox, H. Strack, Ohmic contacts for GaAs devices // *Solid-State Electron.* **10**(12), p. 1213-1218 (1967).

© 2014, V. Lashkaryov Institute of Semiconductor Physics, National Academy of Sciences of Ukraine